Available online at www.sciencedirect.com
SCIENCE DIRECT®
Coastal Engineering 50 (2004) 85–95
Coastal Engineering
An International Journal for Coastal, Harbour and Offshore Engineers
www.elsevier.com/locate/coastaleng

A parabolic equation based on a rational quadratic approximation for surface gravity wave propagation

Soumia Mordane*, Ghita Mangoub, Kamal L. Maroihi, Mohamed Chagdali

Laboratoire de Calcul Scientifique en Mécanique (LCSM), Dept. de Physique, Faculté des Sciences Ben M'Sik, Universite Hassan II Mohammedia, Av. Cdt D El Harti, BP 7955 Casablanca, Morocco

Received 21 January 2003; received in revised form 20 July 2003; accepted 15 September 2003

Abstract

In this work, we are interested in the parabolic formulation of the propagation equation of surface gravity waves in terms of angular capability with respect to the privileged propagation direction. This parabolic formulation is obtained by splitting the Berkhoff equation operator into two parabolic operators representing progressive and reflected wave propagation. The use of the quadratic rational approximation permits to derive simultaneously parabolic equations for transmitted and reflected waves. Two well-known reference examples, which represent the propagation of surface gravity waves when a caustic occurs, will be studied numerically and results will be compared with those of the literature.

Keywords: Wave propagation; Mild slope; Parabolic method; Splitting; Quadratic Padé approximants; Diffraction–refraction

1. Introduction

The method of the parabolic equation has been introduced to the study of surface gravity waves propagation by Liu and Mei (1976) and Radder (1979) and, since that, it has been proven through the contribution of several authors to be an effective model for dealing rapidly and accurately with propagation problems in coastal areas. Basically, this method transforms the Berkhoff elliptic boundary problem (Berkhoff, 1973), which takes into account simultaneously refraction and diffraction effects, into a parabolic initial value problem. This method, leading to an approximation of the equation of Berkhoff (1973), implies that all major components of the wave field must be confined in a narrow angle range centred on a prechosen principal propagation direction.

The equation of Radder (1979) has been widely used, providing the basis of several scientific or commercial codes. The technique of Radder (1979) consists into separating the velocity potential on the free surface into a progressive and a regressive potential. It has been shown by Doïkas (1990) that the resulting equation remains valid for propagation

* Corresponding author.
E-mail addresses: mordane.soumia@caramail.com (S. Mordane), m-chagdali@hotmail.com (M. Chagdali).

0378-3839/$ - see front matter © 2003 Elsevier B.V. All rights reserved.
doi:10.1016/j.coastaleng.2003.09.001

angles within a cone of angles of $\pm 30°$ about the prechosen direction of propagation. Booij (1981) has given, using a splitting technique, a variant of the parabolic approximation of Berkhoff's equation, for which Kirby (1986) gave a justification based on Padé approximants. This equation has been found capable of reproducing the propagation up to an angle of 50° by Lajoie (1996). However, using a criterion based on evaluating a maximal propagating angles from the graphic, Kirby stated that for an error of 5%, this equation is valid up to 55.9°, whereas for an error of 10%, it is valid up to 61.5°.

In this work and in the framework of mild-slope Berkhoff's equation, we develop a parabolic model based on a splitting method that is different from the one of Booij (1981). The equation of Berkhoff is at first transformed into an Helmholtz equation using a scaling factor (Radder, 1979). The operator of this equation is split into a product of two parabolic operators, the first representing reflected waves (back-reflected waves) and the second transmitted waves (progressive waves), containing both of them a square root operator of type $\sqrt{1+X}$, where X is a second-order differential operator called "orthogonal operator". Only the transmitted wave operator is kept. We approximate the operator $\sqrt{1+X}$ by a quadratic rational function, obtaining thus a mixed fifth-order partial differential equation with variable coefficients. We present an implicit finite-difference approximation scheme for its solution. The computational code is built in such a way that computations with a linear rational function may be automatically performed.

We present an exact criterion for determining the maximum propagation angle associated with a given equation, and discuss the dispersion angle associated with the equation we present in comparison with equations cited above. The good performance of the quadratic parabolic wave equation is proved by comparing with well-known reference examples. The comparison will be made with experimental data (Berkhoff et al., 1982; Vincent and Briggs, 1989), equation of Radder (1979), rational linear parabolic equation (Kirby, 1986), and solutions of the equation of Berkhoff (Lajoie, 1996).

2. Theoretical formulation

The propagation of linear, periodic surface waves over a seabed of mild slope is governed by the equation of Berkhoff (1973):

$$\vec{\nabla}_h \cdot (CCg\,\vec{\nabla}\phi) + \frac{\omega^2 Cg}{C}\phi = 0 \tag{1}$$

$\phi(x,y)$ is the complex bidimensional potential function, $\nabla_h \equiv (\partial/\partial x, \partial/\partial y)$ is the horizontal gradient operator and ω is the angular frequency. C and Cg are the corresponding local phase and group velocities of the wave field.

Introducing the scaling factor

$$\varphi = \sqrt{CCg}\,\phi. \tag{2}$$

into Berkhoff's equation yields the Helmholtz equation

$$\nabla^2\varphi + k^2\varphi = 0, \tag{3}$$

where

$$k^2 = k_0^2 - \frac{\nabla^2 (CCg)^{\frac{1}{2}}}{(CCg)^{\frac{1}{2}}}. \tag{4}$$

k_0 is the wave number that verifies locally the dispersion relation $\omega^2 = gk_0\tanh(k_0h)$, h being the local depth and g the gravity. The local phase and group velocities C and Cg are given by $C = \omega/k_0$ and $C_g = \partial\omega/\partial k_0$, respectively.

Eq. (3) may be written in the operator form:

$$\left(\frac{\partial^2}{\partial x^2} + \frac{\partial^2}{\partial y^2} + k^2\right)\varphi = 0 \tag{5}$$

If we assume that the differential operators $\partial/\partial x$ and $(1/k^2)\partial^2/\partial y^2$ commute, the operator of the preceding equation may be factored to give

$$\left(\frac{\partial}{\partial x} + ik\sqrt{1+X}\right)\left(\frac{\partial}{\partial x} - ik\sqrt{1+X}\right)\varphi = 0, \tag{6}$$

where X, the orthogonal operator, is given by

$$X = \frac{1}{k^2}\frac{\partial^2}{\partial y^2}.$$

The first term represents reflected waves (back-reflected waves) and the second term represents progressive waves (transmitted waves). If we remain within the framework of mild-slope Berkhoff's equation, the dispersion relation cited above is valid and we can, in good approximation, consider that the operator $\partial/\partial x$ and $(1/k^2)\partial^2/\partial y^2$ commute which amounts $\partial k/\partial x \ll k^2$. If we assume that waves propagate without significant back reflection, which is the case for the propagation from offshore to inshore, Eq. (6) reduces to

$$\left(\frac{\partial}{\partial x} - ik\sqrt{1+K}\right)\varphi = 0. \tag{7}$$

Different approximation of $\sqrt{1+X}$ lead to different parabolic equations. The most classical approximation is the development in Taylor series:

$$\sqrt{1+X} \approx 1 + \frac{X}{2} - \frac{X^2}{8} + \frac{X^3}{16} \cdots. \tag{8}$$

The first two terms lead to the equation of Radder (1979) on a flat seabed, and the first three terms lead to the equation of Kirby (1986), valid also on a flat seabed, for which angular capability (70°) encompasses the equation of Radder (1979). It is then obvious that using more and more terms of the series will improve progressively the angular capability. However, the parabolic equations based on this approximation remain relatively inefficient. Indeed, some topographic configurations need to take into account many terms of the series, which make their implementation difficult because of the rising powers of the operator X. The rational function approximation permits to improve the angular capability considerably by summing relatively few terms with regard to Taylor series. In the present paper, we have chosen a quadratic rational function which writes

$$\sqrt{1+X} \cong \frac{P_1 + P_2X + P_3X^2}{q_1 + q_2X + q_3X^2} + o(X^5) \tag{9}$$

where the p_i and q_i are Padé coefficients and

$$X^2 = \frac{2}{k^5}\left(\frac{3}{k}\left(\frac{\partial k}{\partial y}\right)^2 - \frac{\partial^2 k}{\partial y^2}\right)\frac{\partial^2}{\partial y^2} - \frac{4}{k^5}\frac{\partial k}{\partial y}\frac{\partial^3}{\partial y^3} + \frac{1}{k^4}\frac{\partial^4}{\partial y^4}.$$

Now, applying this fourth-order Padé approximation in Eq. (7), one obtains the new pseudo-partial differential equation

$$\frac{\partial \phi}{\partial x} = ik\frac{P_1 + P_2X + P_3X^2}{q_1 + q_2X + q_3X^2}\phi. \tag{10}$$

If we operate formally on the latter equation with $q_1 + q_2X + q_3X^2$, then we obtain

$$(q_1 + q_2X + q_3X^2)\frac{\partial \phi}{\partial x} = ik(P_1 + P_2X + P_3X^2)\phi. \tag{11}$$

Using the expressions of X and X^2, Eq. (11) becomes

$$\left(\alpha_1 + \alpha_2\frac{\partial^2}{\partial y^2} + \alpha_3\frac{\partial^3}{\partial y^3} + \alpha_4\frac{\partial^4}{\partial y^4}\right)\frac{\partial \phi}{\partial x} = ik\left(\beta_1 + \beta_2\frac{\partial^2}{\partial y^2} + \beta_3\frac{\partial^3}{\partial y^3} + \beta_4\frac{\partial^4}{\partial y^4}\right)\phi, \tag{12}$$

where $\alpha_1 = q_1$; $\alpha_2 = (q_2/k^2) + (2q_3/k^5)[(3/k)(\partial k/\partial y)^2 - (\partial^2 k/\partial y^2)]$; $\alpha_3 = -(4q_3/k^5)(\partial k/\partial y)$; $\alpha_4 = (q_3/k^4)$; $\beta_1 = p_1$; $\beta_2 = (p_2/k^2) + (2p_3/k^5)[(3/k)(\partial k/\partial y)^2 - (\partial^2 k/\partial y^2)]$; $\beta_3 = -(4p_3/k^5)(\partial k/\partial y)$; $\beta_4 = (p_3/k^4)$. Eq. (12) is a fifth-order partial differential parabolic equation with variable coefficients. This equation may be used to model the propagation at very wide propagation angles; the propagation in an environment where the wave number k varies substantially as a function of space; and the propagation in very large areas of several wavelengths. In the present form, Eq. (12) is intrinsically implicit and we shall apply a Crank–Nicolson method to solve it. For propagation problems involving a flat seabed, coefficients of Eq. (12) need to be calculated only once. When the seabed is variable, these coefficients must be recalculated at each x where the wave

number varies or regularly at each x increment if the seabed varies continuously.

The obtained equation is of the parabolic type. It contains all equations cited above as special cases: the set Pr=$\{p_1=1, p_2=1/2, p_3=0, q_1=1, q_2=0, q_3=0\}$ leads to the equation of Radder (1979) on a flat seabed, and the set Pk=$\{p_1=1, p_2=3/4, p_3=0, q_1=1, q_2=1/4, q_3=0\}$ leads to the equation of Kirby (1986). There are several methods to obtain a given set of coefficients $\{p_1, p_2, p_3, q_1, q_2, q_3\}$. The set Pa=$\{p_1=1, p_2=5/4, p_3=5/16, q_1=1, q_2=3/4, q_3=1/16\}$ is obtained by requiring that the rational function and its four first derivatives coincide with those of the operator function $\sqrt{1+X}$ at $X=0$. The set Pkni=$\{p_1=1.628909, p_2=2.428289, p_3=0.8308198, q_1=1.628934, q_2=1.615038, q_3=0.235499\}$ is obtained using an ad hoc technique of Chebychev (St. Mary, 1985).

3. Angular capability

It has been shown that the angular capability of Radder's equation is 30° (Doïkas, 1990; Lajoie, 1996). We shall establish a criterion which uses this result in order to determinate the maximal propagation angle that one can associate to a given equation. Consider the case of the plane wave propagating over a flat seabed (k=constant). Solutions of the wave equation are in this case

$$\exp[\pm ik(k_x x \pm k_y y)] \tag{13}$$

where k_x, cosine of the propagation angle θ measured with respect to the privileged propagation direction, and k_y, its sinus, verify the exact relation

$$k_x^2 + k_y^2 = 1,$$

or

$$k_x = \pm\sqrt{1-k_y^2} \tag{14}$$

Solutions (13) are used to derive the approximate k_x for the parabolic quadratic equations:

$$k_x = \pm(p_1 - p_2 k_y^2 + p_3 k_y^4)/(q_1 - q_2 k_y^2 + q_3 k_y^4). \tag{15}$$

Using respectively the sets Pr and Pk in Eq. (15), we get the approximate k_x for the parabolic equation of Radder (1979):

$$k_x = \pm(1 - k_y^2/2),$$

and of Kirby (1986):

$$k_x = \pm\left(1 - \frac{3}{4}k_y^2\right) \Big/ \left(1 - \frac{1}{4}k_y^2\right).$$

We define the error $\tau(\theta)$ by $\tau(\theta) = |k_{xe}(\theta) - k_{xa}(\theta)|$. We associate then as a maximal propagation angle to a

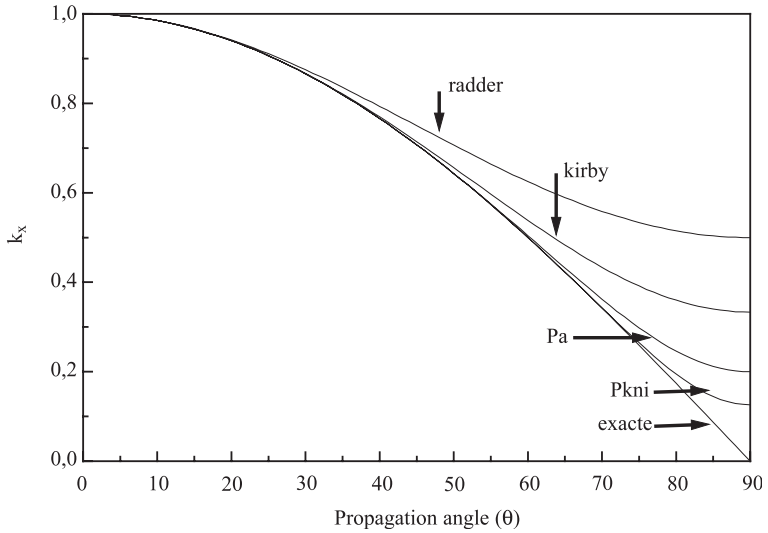

Fig. 1. Variation of k_x with the propagation angle θ.

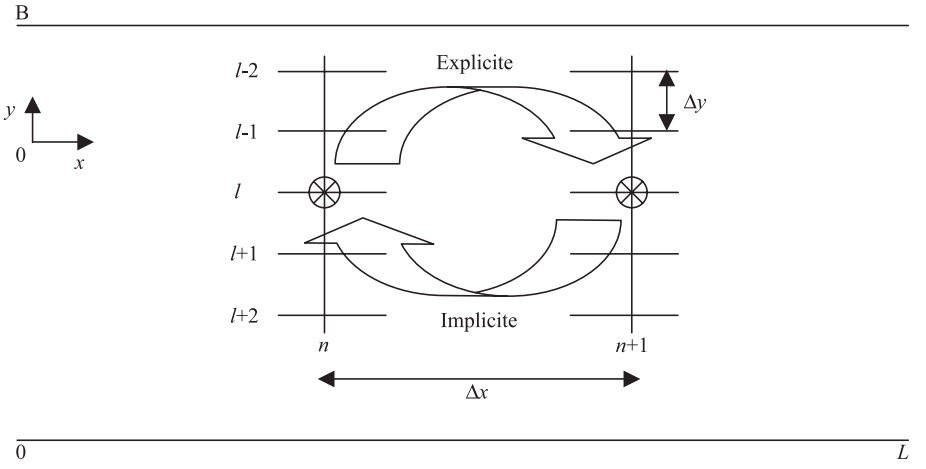

Fig. 2. The propagation domain of the study.

given equation the most large angle for which τ is less or equal to its value at $\theta = 30°$ for the equation of Radder ($\tau_{30} = 0.009$). This criterion permits to associate an angle of 47° to the equation of Kirby (1986) instead of 50°, of 65° to the quadratic parabolic Eq. (15) with the set Pa, and of 77° to the quadratic parabolic Eq. (15) with the set Pkni. These maximal propagation angles may also be determinated approximately from the graphic of Fig. 1 which presents exact and approximate k_x as a function of the propagation angle θ. Since the angular capability of the Pkni coefficients encompass the one of the Pa coefficients, we shall use the Pkni set for our numerical computations.

4. Numerical solution

The domain of propagation we use to carry out our numerical experiments is depicted in Fig. 2. It is a rectangular wave guide of length L and width B that are constants. The depth h is variable ($h = h(x,y)$). The lateral boundaries, perpendicular boundaries to the privileged direction of propagation, are rigid. The boundary conditions on these boundaries and their numerical treatment are given in the next section.

We choose for the discretization a standard rectangular grid. The constant space steps are denoted Δx and Δy for directions x and y, respectively. M is an integer such as $M = B/\Delta y$. The integers n and l are used respectively as indexes on variables x and y. Thus, y_0 and y_M correspond to the lateral boundaries. For $x_n = n\Delta x$ and $y_l = l\Delta y$, we let $\phi(x_n,y_l) = \phi_l^n$.

We apply to Eq. (12) a standard Crank–Nicolson scheme for traditional parabolic partial differential equations. Namely, we take the average of the classical explicit (forward) difference approximation based at the point (x_n,y_l) and the (backwards) implicit approximation based at (x_{n+1},y_l) (cf. Fig. 2). The resulting discretized equation is

$$\begin{aligned} a1_l^n\phi_{l-2}^{n+1} + b1_l^n\phi_{l-1}^{n+1} + c1_l^n\phi_l^{n+1} + d1_l^n\phi_{l+1}^{n+1} + e1_l^n\phi_{l+2}^{n+1} \\ = a0_l^n\phi_{l-2}^n + b0_l^n\phi_{l-1}^n + c0_l^n\phi_l^n + d0_l^n\phi_{l+1}^n \\ + e0_l^n\phi_{l+2}^n, \end{aligned} \tag{16}$$

$l = 0,1,2,\ldots,M$; $n = 1,2,\ldots,n_{\max}$. The different coefficients involved in Eq. (16) are given by

$$\begin{aligned} a0_l^n = &-\frac{1}{4\Delta y^3}[(\alpha_3)_l^{n+1} + (\alpha_3)_l^n + ik_l^n\Delta x(\beta_3)_l^n] \\ &+ \frac{1}{\Delta y^4}[(\alpha_4)_l^{n+1} + (\alpha_4)_l^n + ik_l^n\Delta x(\beta_4)_l^n]; \end{aligned}$$

$$\begin{aligned} b0_l^n = &\frac{1}{2\Delta y^2}[(\alpha_2)_l^{n+1} + (\alpha_2)_l^n + ik_l^n\Delta x(\beta_2)_l^n] \\ &+ \frac{1}{2\Delta y^3}[(\alpha_3)_l^{n+1} + (\alpha_3)_l^n + ik_l^n\Delta x(\beta_3)_l^n] \\ &- \frac{2}{\Delta y^4}[(\alpha_4)_l^{n+1} + (\alpha_4)_l^n + ik_l^n\Delta x(\beta_4)_l^n]; \end{aligned}$$

$$c0_l^n = \alpha_1 + \frac{ik_l^n \Delta x}{2}\beta_1 - \frac{1}{\Delta y^2}[(\alpha_2)_l^{n+1} + \alpha_2)_l^n + ik_l^n \Delta x \beta_2)_l^n] + \frac{3}{\Delta y^4}[(\alpha_4)_l^{n+1} + \alpha_4)_l^n + ik_l^n \Delta x \beta_4)_l^n];$$

$$d0_l^n = \frac{1}{2\Delta y^2}[(\alpha_2)_l^{n+1} + \alpha_2)_l^n + ik_l^n \Delta x \beta_2)_l^n] - \frac{1}{2\Delta y^3} \times [(\alpha_3)_l^{n+1} + \alpha_3)_l^n + ik_l^n \Delta x \beta_3)_l^n] - \frac{2}{\Delta y^4}[(\alpha_4)_l^{n+1} + \alpha_4)_l^n + ik_l^n \Delta x \beta_4)_l^n];$$

$$e0_l^n = +\frac{1}{4\Delta y^3}[(\alpha_3)_l^{n+1} + \alpha_3)_l^n + ik_l^n \Delta x \beta_3)_l^n] + \frac{1}{2\Delta y^4} \times [(\alpha_4)_l^{n+1} + \alpha_4)_l^n + ik_l^n \Delta x \beta_4)_l^n];$$

$$a1_l^n = -\frac{1}{4\Delta y^3}[(\alpha_3)_l^{n+1} + \alpha_3)_l^n - ik_l^{n+1} \Delta x \beta_3)_l^{n+1}] + \frac{1}{\Delta y^4}[(\alpha_4)_l^{n+1} + \alpha_4)_l^n - ik_l^{n+1} \Delta x \beta_4)_l^{n+1}];$$

$$b1_l^n = \frac{1}{2\Delta y^2}[(\alpha_2)_l^{n+1} + \alpha_2)_l^n - ik_l^{n+1} \Delta x \beta_2)_l^{n+1}] + \frac{1}{2\Delta y^3} \times [(\alpha_3)_l^{n+1} + \alpha_3)_l^n - ik_l^{n+1} \Delta x \beta_3)_l^{n+1}] - \frac{2}{\Delta y^4} \times [(\alpha_4)_l^{n+1} + \alpha_4)_l^n - ik_l^{n+1} \Delta x \beta_4)_l^{n+1}];$$

$$c1_l^n = \alpha_1 - \frac{ik_l^{n+1} \Delta x}{2}\beta_1 - \frac{1}{\Delta y^2}[(\alpha_2)_l^{n+1} + \alpha_2)_l^n - ik_l^{n+1} \Delta x \beta_2)_l^{n+1}] + \frac{3}{\Delta y^4}[(\alpha_4)_l^{n+1} + \alpha_4)_l^n - ik_l^{n+1} \Delta x \beta_4)_l^{n+1}];$$

$$d1_l^n = \frac{1}{2\Delta y^2}[(\alpha_2)_l^{n+1} + \alpha_2)_l^n - ik_l^{n+1} \Delta x \beta_2)_l^{n+1}] - \frac{1}{2\Delta y^3} \times [(\alpha_3)_l^{n+1} + \alpha_3)_l^n - ik_l^{n+1} \Delta x \beta_3)_l^{n+1}] - \frac{2}{\Delta y^4} \times [(\alpha_4)_l^{n+1} + \alpha_4)_l^n - ik_l^{n+1} \Delta x \beta_4)_l^{n+1}];$$

$$e1_l^n = +\frac{1}{4\Delta y^3}[(\alpha_3)_l^{n+1} + \alpha_3)_l^n - ik_l^{n+1} \Delta x \beta_3)_l^{n+1}] + \frac{1}{2\Delta y^4}[(\alpha_4)_l^{n+1} + \alpha_4)_l^n - ik_l^{n+1} \Delta x \beta_4)_l^{n+1}].$$

The appearance of five unknowns in the general Eq. (16) indicates that the matrix system to invert is penta-diagonal.

5. Boundary conditions and matrix formulation

The lateral boundaries being rigid, the boundary conditions for Helmholtz equation are given by

$$\frac{\partial \phi}{\partial y}(x, y_0) = 0, \quad \frac{\partial \phi}{\partial y}(x, y_M) = 0. \tag{17}$$

It is important to translate the boundary conditions (17) related to the second-order derivatives in y into corresponding ones for the fourth-order Eq. (12). Since conditions (17) hold for any x, all higher derivatives with respect to x of $\partial/\partial y$ at y_0 and y_M are equal to 0. It follows by differentiating Eq. (5) with respect to y and using conditions (17) that

$$\frac{\partial^3 \phi}{\partial y^3}(x, y_0) = 0, \quad \frac{\partial^3 \phi}{\partial y^3}(x, y_M) = 0 \tag{18}$$

for all x. Thus, in addition to basic boundary conditions (17), we have inherited boundary conditions (18).

For the discretization, we introduce the fictitious points ϕ_{-2}^n, ϕ_{-1}^n, ϕ_{M+1}^n and ϕ_{M+2}^n. Using a central finite difference to discretize conditions (17), one obtain $\phi_{-1}^n = \phi_1^n$ and $\phi_{m+1}^n = \phi_{M-1}^n$ for any n. It then follows on approximating conditions (18) by a central difference that $\phi_{-2}^n = \phi_2^n$ and $\phi_{M+2}^n = \phi_{M-2}^n$ for any n.

It is obvious from the discretization of boundary conditions (17) and (18) that the two first and the two

last lines of the matrix system must be modified in order to take into account the boundary conditions. The general matrix system form is then

$$A1^{(n)}u^{n+1} = A0^{(n)}u^{n},$$

where, for $I=0,1$,

$$AI=\begin{pmatrix} cI_0 & dI_0' & eI_0' & & & & & \\ bI_1 & cI_1' & dI_1 & eI_1 & & & & \\ aI_2 & bI_2 & cI_2 & dI_2 & eI_2 & & & \\ & & \cdots & & & & & \\ & & & \cdots & & & & \\ & & & & \cdots & & & \\ & & & aI_{M-2} & bI_{M-2} & cI_{M-2} & dI_{M-2} & eI_{M-2} \\ & & & & aI_{M-1} & bI_{M-1} & cI_{M-1}' & dI_{M-1} \\ & & & & & aI_M' & bI_M' & cI_M \end{pmatrix}, \quad u^{n+1}=\begin{pmatrix} u_0^{n+1} \\ u_1^{n+1} \\ u_2^{n+1} \\ \vdots \\ u_{M-2}^{n+1} \\ u_{M-1}^{n+1} \\ u_M^{n+1} \end{pmatrix},$$

and $eI_0' = eI_0 + aI_0$; $dI_0' = dI_0 + bI_0$; $cI_1' = cI_1 + aI_1$; $cI'_{M-1} = cI_{M-1} + eI_{M-1}$; $aI'_M = aI_M + eI_M$; $bI'_M = bI_M + dI_M$.

6. Application to an elliptic shoal—example 1

The first studied example is an experimental arrangement that consists of an elliptic shoal resting on a flat bottom topography. The boundary of the elliptic shoal is given by

$$\frac{x^2}{(3.96)^2} + \frac{y^2}{(3.05)^2} = 1,$$

and the depth in the shoal region is modified according to

$$h = 0.9144 - 0.762\sqrt{1 - \frac{x^2}{(4.95)^2} - \frac{y^2}{(3.81)^2}},$$

(x,y) being Cartesian coordinates. Outside the shoal region, the constant depth is 0.457 m.

The propagation of surface gravity waves in this laboratory environment has been studied experimentally by Vincent and Briggs (1989), and investigated numerically by solving the equations of Berkhoff and Radder by Lajoie (1996). The initial wave is monochromatic, normal to the main ellipsoid axis, and has a period $T=1.3$ s. Fig. 3 illustrates the experimental arrangement, which corresponds to the computational domain, along with the labeled transects 1–6 for which data from the laboratory experiment of Vincent and Briggs (1989) are available. The results are presented as plots of normalized wave amplitude with respect to the incident wave amplitude (A/A_0).

Fig. 4-1 is a comparison between results of the equation of Radder, the rational linear approxima-

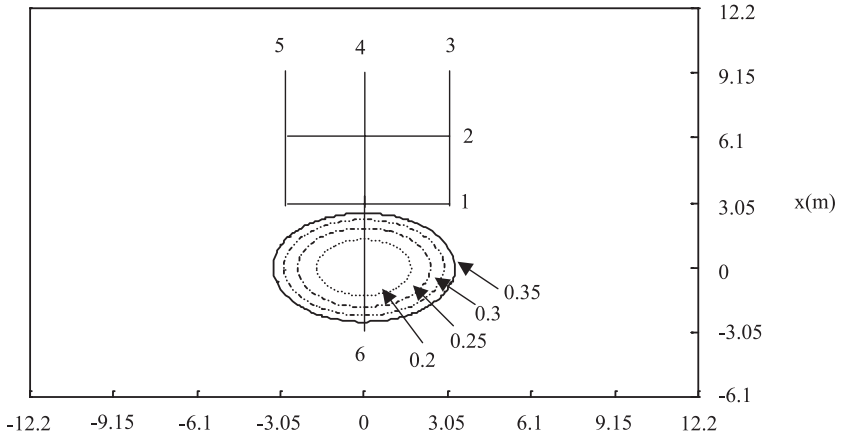

Fig. 3. Bathymetry of the computational domain for the experiment by Vincent and Briggs (1989). Dashed lines indicate the transects of wave measurements.

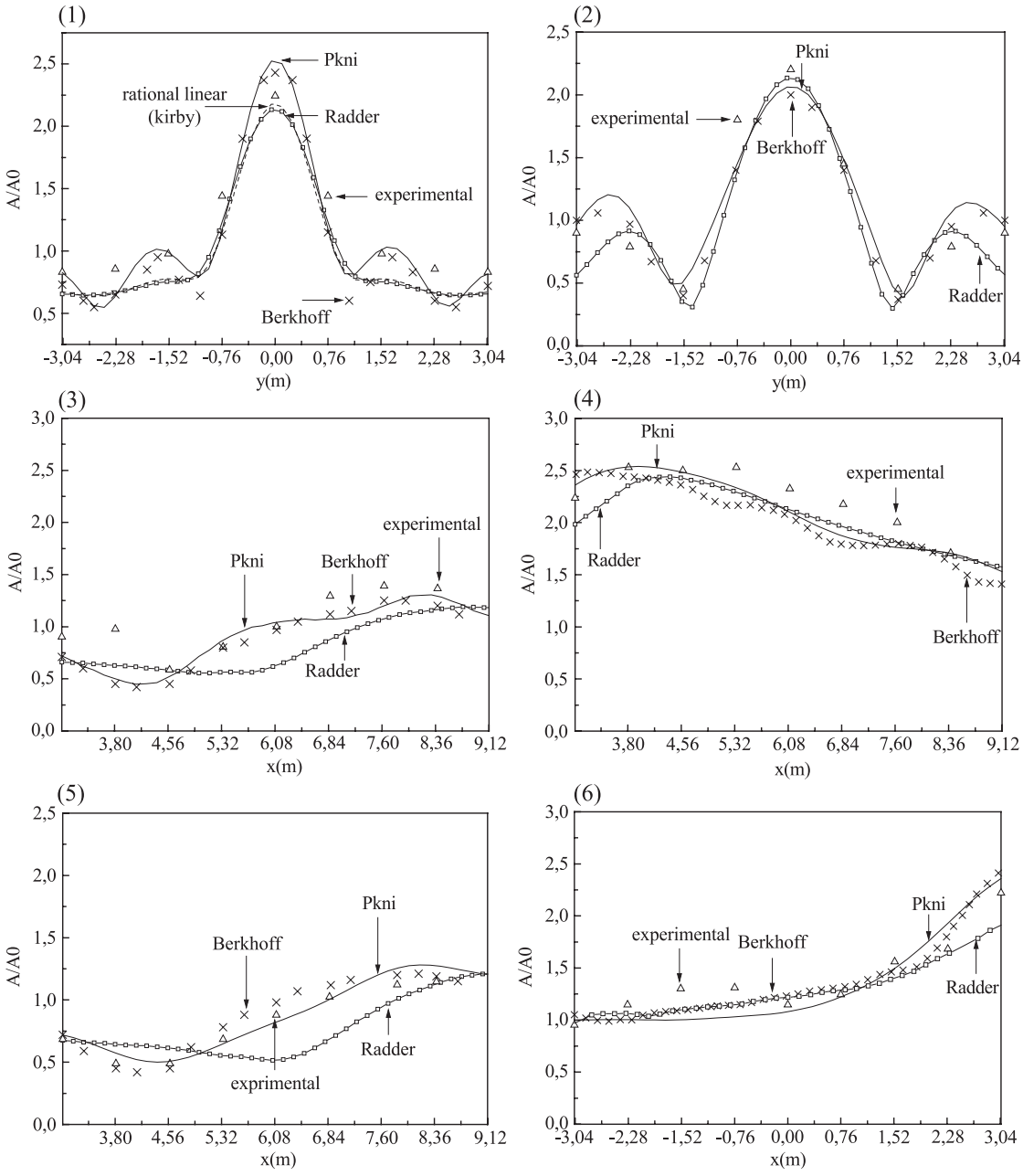

Fig. 4. (1–6) Comparison of the quadratic model results against the results of Radder and Berkhoff equations and experimental data along sections 1–6, respectively (see Fig. 3).

tion of Kirby, the rational quadratic approximation, the solution of the equation of Berkhoff (cf. Lajoie, 1996) and the experimental data. It is obvious that the rational quadratic model fit with higher agreement the experimental data and results by Berkhoff's equation than does the rational linear

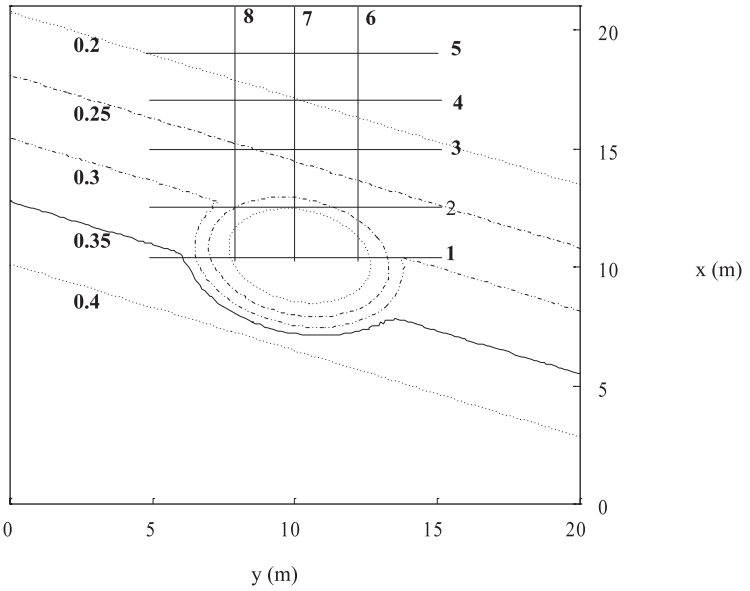

Fig. 5. Bathymetry of the computational domain for the experiment by Berkhoff et al. (1982). Dashed lines indicate the transects of wave measurements.

approximation. Therefore, numerical investigations using the rational linear approximation will not be presented henceforward.

In Fig. 4-2 to 4-6, we compare solutions of the quadratic model, the equations of Radder and Berkhoff and experimental data. All these figures show that results of the quadratic model are in better agreement with experimental data. However, some discrepancy remains due probably to the possible presence of reflected waves in the experimental data. Other reason could be nonlinearity which is not accounted for in the present model. Overhead the shoal, the focusing occurs more rapidly for the quadratic model than for Berkhoff and Radder equations. This is consistent with the trends of the experimental data as it can be seen from Fig. 4-4 and 4-6. Moreover, the fact that the quadratic model fit with agreement the experimental data and the results by Berkhoff's equation outside the focal region (Fig. 4-1 and 4-2) is a proof of it's reliability to represent diffracted waves with very wide propagation angles.

7. Application to an elliptic shoal—example 2

The second studied example is an experimental arrangement that consists of an elliptic shoal resting on a plane sloping bottom with a slope of 1:50. The slope rises from a region of constant depth (0.45 m) near a straight wave paddle, and is rotated clockwise at an angle of 20° from the wave paddle. The slope topography in the absence of the shoal, the boundary of the elliptic shoal and the depth in the shoal region are given respectively by

$$h = \begin{cases} 0.45 \text{ m}, & x' > -5.84 \text{ m} \\ 0.45 - 0.02(5.84 + x') \text{ m}, & x' \geq -5.84 \text{ m} \end{cases}$$

Fig. 6. (1–8) Comparison of the quadratic model results against the results of the linear model of Dalrymple et al. (1989) and experimental data by Berkhoff et al. (1982) along sections 1–8, respectively (see Fig. 5).

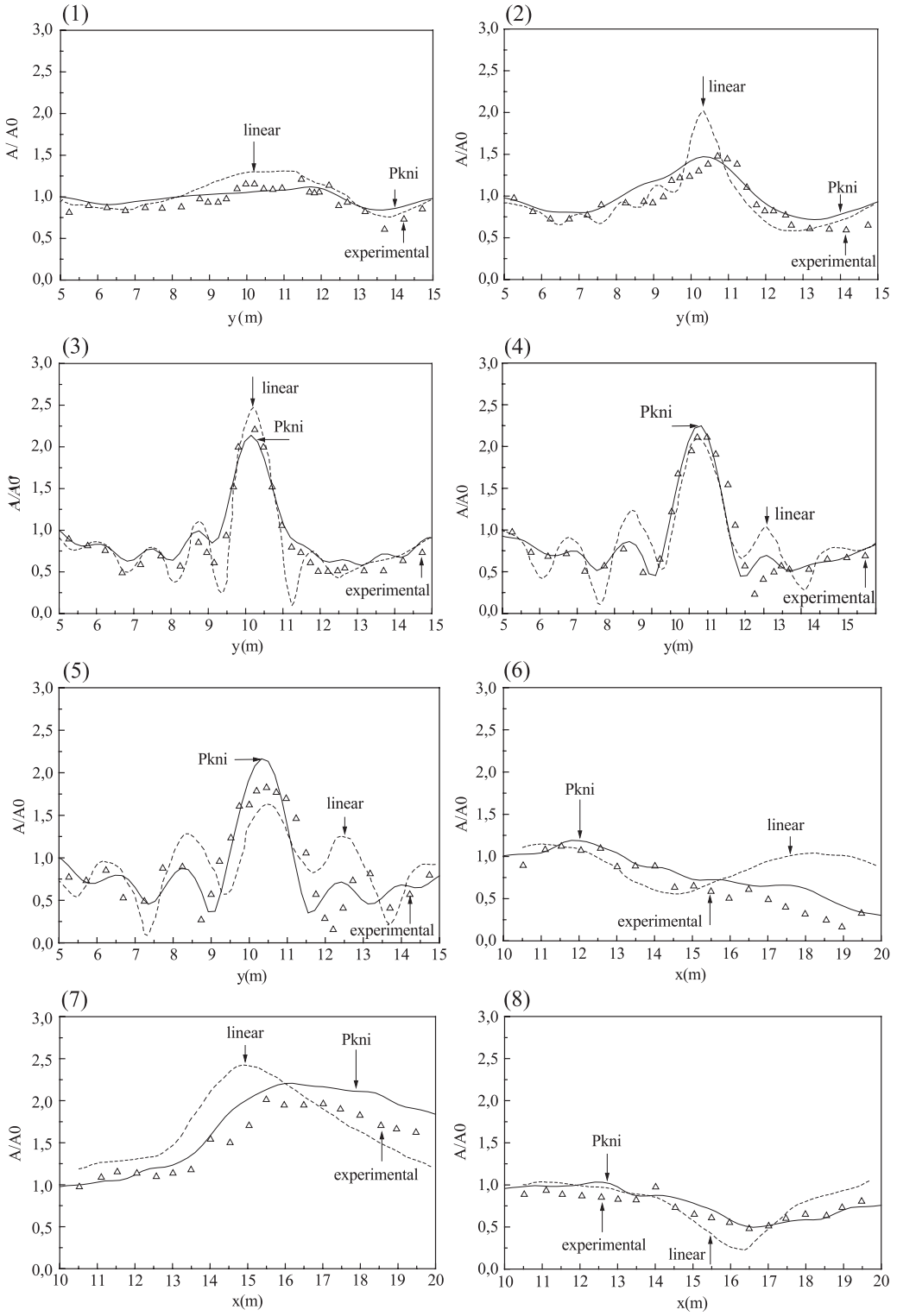
(1)
A/ A0
linear
Pkni
experimental
y(m)
(2)
A/A0
linear
Pkni
experimental
y(m)
(3)
A/A0
linear
Pkni
experimental
y(m)
(4)
A/A0
Pkni
linear
experimental
y(m)
(5)
A/A0
Pkni
linear
experimental
y(m)
(6)
A/A0
Pkni
linear
experimental
x(m)
(7)
A/A0
linear
Pkni
experimental
x(m)
(8)
A/A0
Pkni
experimental
linear
x(m)

Fig. 6.

$$\left(\frac{x'}{3}\right)^2+\left(\frac{y'}{4}\right)^2=1$$

and

$$h=h-0.5\left[1-\left(\frac{x'}{3.75}\right)^2+\left(\frac{y'}{5}\right)^2\right]^{1/2}+0.3,$$

where the slope-oriented coordinates (x',y') are related to the computational Cartesian coordinates by

$$x' = (x-10.5)\cos(20^\circ)-(y-10)\sin(20^\circ)$$

$$y' = (x-10.5)\sin(20^\circ)+(y-10)\cos(20^\circ)$$

The propagation of surface gravity waves in this laboratory environment has been studied experimentally by Berkhoff et al. (1982) and numerically by several authors (Kirby and Dalrymple, 1983; Kirby, 1986; Dalrymple et al., 1989). The initial wave is monochromatic and of period $T=1$ s. Since the depth near the wave paddle is constant, the initial wave corresponds to a uniform wave train generated by the wave paddle. The amplitude of the incident wave is $A_0=0.0232$. Fig. 5 illustrates the experimental arrangement, which corresponds to the computational domain, along with the labeled transects 1–8 for which data from the laboratory experiment of Berkhoff et al. (1982) are available.

Fig. 6-1 to 6-8 presents results obtained by the quadratic model, those obtained by Dalrymple et al. (1989) using their linear model, along with experimental data of Berkhoff et al. (1982). As it can be seen from the whole of the figures, we find that the quadratic model results are in very closer agreement with experimental data than do the results of the linear model (Dalrymple et al., 1989). This fact reassures the reliability of the quadratic model to reproduce diffracted waves with very wide propagation angles.

8. Conclusion

In the present paper, we have presented a wide-angle parabolic equation for dealing with surface gravity waves propagation. It is based on a splitting technique that is different from the one proposed by Radder (1979) and Booij (1981). This method yields two parabolic equations for the transmitted and reflected waves, and the parabolic equation is obtained by neglecting reflected waves. The discrete equation results in a five-diagonal linear system to which we apply an easily implemented penta-diagonal solver that is comparable in running time to tri-diagonal solvers. We demonstrated in two test situations that this higher-order equation and associated equations are accurate at very wide propagation angles.

References

Berkhoff, J.C.W., 1973. Computation of combined refraction–diffraction. Proceedings of the 13th Coastal Engineering Conference, Vancouver (Canada) ASCE, USA, pp. 471–490.

Berkhoff, J.C.W., Booij, N., Radder, A.C., 1982. Verification of numerical wave propagation models for simple harmonic linear waves. Coast. Eng. 6, 255–279.

Booij, N., 1981. Gravity waves on water with non-uniform depth and current. Rep. 81-1, Dep. Of Civil Engineering, Delft University of Technology., Delft.

Dalrymple, R.A., Suh, K.D., Kirby, J.T., Chae, J.W., 1989. Models for very wide-angle water waves and wave diffraction: Part 2. Irregular bathymetry. J. Fluid Mech. 201, 299–322.

Doïkas, S., 1990. Propagation de la houle au voisinage de la côte. Mise au point des codes numériques en différences finies. Thèse d'Université, Paris Sud.

Kirby, J.T., 1986. Higher-order approximations in parabolic equation method for water waves. J. Geophys. Res. 91, 933–952.

Kirby, J.T., Dalrymple, R.A., 1983. A parabolic equation for the combined refraction–diffraction of Stokes waves by mildly varying topography. J. Fluid Mech. 136, 453–466.

Lajoie, D., 1996. Modélisation de la houle en zone côtière: Prévision de l'agitation à l'intérieur des ports et mise au point d'atténuateurs de houle dynamiques. Thèse de l'université d'Aix-Marseille II.

Liu, P.L.F., Mei, C.C., 1976. Water motion on a beach in the presence of a breakwater: 1. Waves. J. Geophys. Res. 81, 3079–3084.

Radder, A.C., 1979. On the parabolic equation method for water-wave propagation. J. Fluid Mech. 95, 159–176.

St. Mary, D.F., 1985. Analysis of an implicit finite difference scheme for very wide angle underwater acoustic propagation. Proceedings of the 11th IMACS World Congress on system simulation and scientific computation, Oslo (Norway), vol. 2, pp. 153–156.

Vincent, C.L., Briggs, M.J., 1989. Refraction–diffraction of irregular waves over a mound. J. Waterw. Port Coast. Ocean Eng., ASCE 115 (2), 269–284.